

Nanosecond Raman scattering computation in large plasmas

Olivier Morice, Michel Casanova

*Commissariat à l'énergie atomique, centre DAM Île-de-France, Bruyères-le-Châtel, 91297
Arpajon Cedex, France*

Introduction

Laser-plasma interaction (LPI) might be one of the main limiting processes involved in the operating of high power laser facilities such as the *ligne d'intégration laser* (LIL) or the future *laser Mégajoule* (LMJ) [1]. Among the various LPI physical effects, Raman backscattering in nanosecond regime is probably the most complicated to understand and to predict. There are many difficulties involved by the Raman scattering, such as the large number of physical regimes, as well as the general multi-scale behavior of this instability. More precisely, LMJ-relevant regime corresponds to values of $k_{Lm}\lambda_{De} > 0.3$ (k_{Lm} being the Langmuir wave wavenumber and λ_{De} the Debye length) in which kinetic phenomena in saturation regime have to be dealt with, together with space and time large scale variations of hydrodynamic parameters. We furthermore note that such regimes are, for a given electron density, difficult to achieve on smaller laser experiments.

Let us first note that our goal of simulating full LMJ (centimeter sized) cavities is hardly achievable. We thus for now restrict ourselves to an LPI devoted millimeter-sized experiment, which should be achieved on the LIL facility during the current year. As we already presented in previous conferences [2, 3], we first use a 2D Lagrangian and ray-tracing code (FCI2) to compute the plasma parameters profile within the whole geometry of the experiment. We subsequently carry out specific linear and nonlinear Raman calculations within a delimited space and time area of the experiment (mesoscopic scale). These specific calculations use FCI2 results as initial conditions.

LPI devoted experiment on the LIL facility

An experimental campaign devoted to LPI is being carried out on the LIL facility to achieve LMJ-like conditions. We used for our theoretical studies the parameters of one of these experiments, although the corresponding experimental results are not yet available. Scheme of the experiment and corresponding hydrodynamic simulations results are presented on figure 1. The setup is constituted by a 4 mm length and 1.4 mm diameter gold tube, filled with pentane gas and closed by two plastic windows. The laser (14 kJ, 6 ns at $\lambda = 351$ nm) first destroys the windows, then heats the pentane, and a density plateau at about $n_e/N_c = 0.15$ with a 3 keV

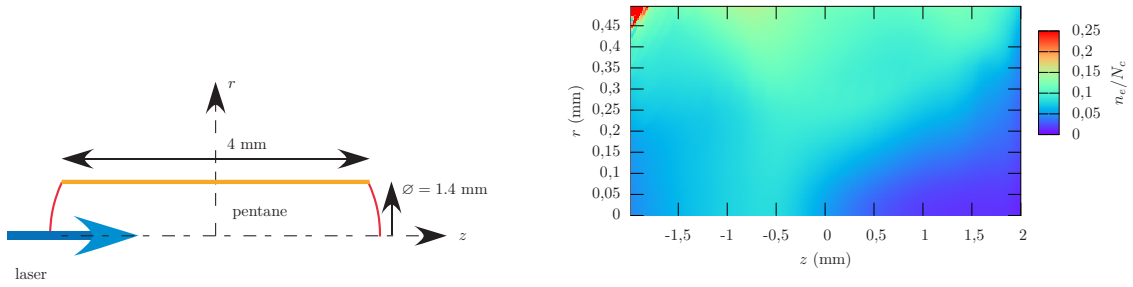


Figure 1: Hydrodynamic simulation of a LPI-devoted experiment on the LIL facility. The left is the experimental scheme, the right the plasma density profile after 4.1 ns.

electron temperature is obtained after 4.1 ns.

Linear Raman calculations

Linear gain for Raman scattering can be evaluated using the following formula:

$$G = \int_0^z dz' \left\{ \frac{1}{\omega_s v_{gs}} \left(\frac{q_e k_p}{m_e} \right)^2 \Im \frac{\chi_e (1 + \chi_i)}{\epsilon} |\vec{A}_L|^2 - \frac{2v_{coll}}{v_{gd}} \right\}. \quad (1)$$

where the indexes s and p stand for the scattered and plasma waves, and $|\vec{A}_L|^2$ is the vector potential related to the laser intensity. The latter is calculated from using the envelope profile of a diffracting speckle pattern [4]. Since the G factor is actually the argument of an exponent which characterizes the amplification of thermal noise, one usually considers that the Raman scattering is relevant when G exceeds a factor of about 20. Figure 2 presents for the LIL plasma ($t = 4.1$ ns) the linear gains corresponding to backward and to forward Raman scattering. One finds that both should be significant.

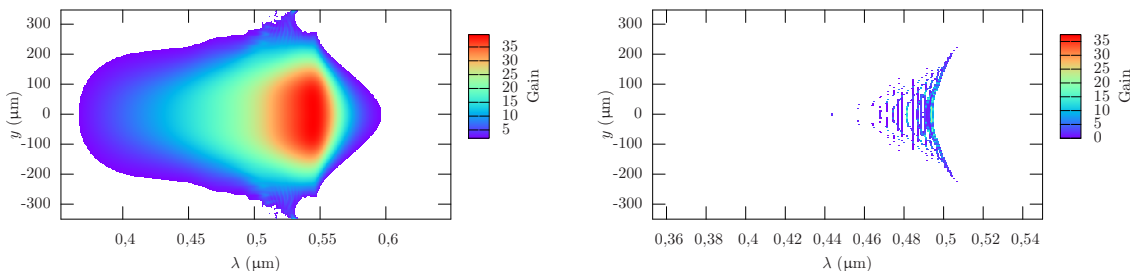


Figure 2: Linear gain for backward (on the left) and forward Raman scattering (on the right), in case of the LIL plasma, for $t = 4.1$ ns and as a function of the scattered wavelength and the transverse direction.

In formula (1) the integration is carried out along lines parallel to the z axis. Furthermore, a linear computation of Raman scattering is possible together with dealing with the multidimensional geometry of the plasma. For that purpose, we propagate independently the scattered

frequencies taking into account the amplification factor inside the braces in equation (1). Processing starts from thermal noise locate both on scattered light and on electron density fluctuations. Resulting scattered spectra can be compared to gain value. The observed dependance with the dimension can be explained by geometrical considerations.

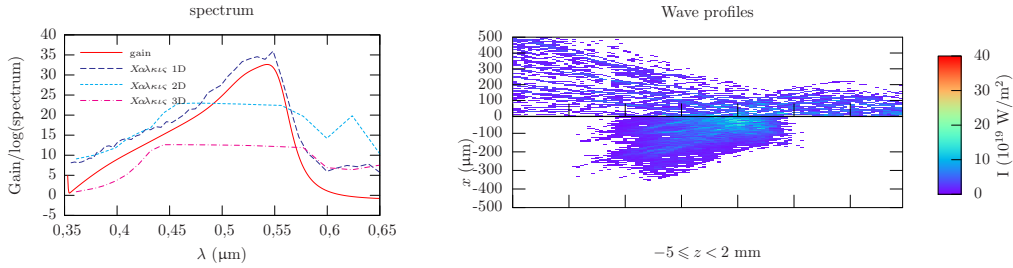


Figure 3: Linear multidimensional Raman processing within the LIL plasma. On the left, comparison of the theoretical gain value (eq. 1) and the computed spectra for each dimension values. On the right, pump (upper side) and backscattered Raman (lower side) profiles for a 2D calculation.

Nonlinear Raman calculations

Previously presented linear calculation may provide efficient predictions of scattered light spectra, but cannot compute levels of reflectivity since nonlinear effects are not dealt with. This problem is very complicated since kinetic effects are involved in the regimes of large $k_{Lm}\lambda_{De}$ we study. We for now restrict ourselves to a very simplified approach in which all the waves involved by the process (electromagnetic and electrostatic) are modeled by an envelop (paraxial) approximation. The coefficients of these envelop equations are deduced from linear kinetic plasma theory. In addition to the pump depletion, we tried to deal with some nonlinear kinetic effects by adding nonlinear shifts, deduced either from Morales & O'Neil [5] or from adiabatic [6] theories. We did not however, in case of our plasma parameters, notice some relevant effect of these nonlinear shifts.

More dramatic was in our case the broadband effects related to the variation range of the electron density (typically from 0 to $0.15 N_c$). These density variations are responsible of a shortening of the time of coherence of the scattered light (typically of the order of the femtosecond). A rigorous treatment of such a situation would need large amount of discretization steps, both in space and time, and would reach the limits of validity of the paraxial theory. To overcome this problem, we slightly modified the envelop equation model by adding a space dependence of the frequency and the wavevector, and allowing ourselves to remove progressively the off-resonant part of the light [3]. This kind of trick allowed us to produced reflectivity and

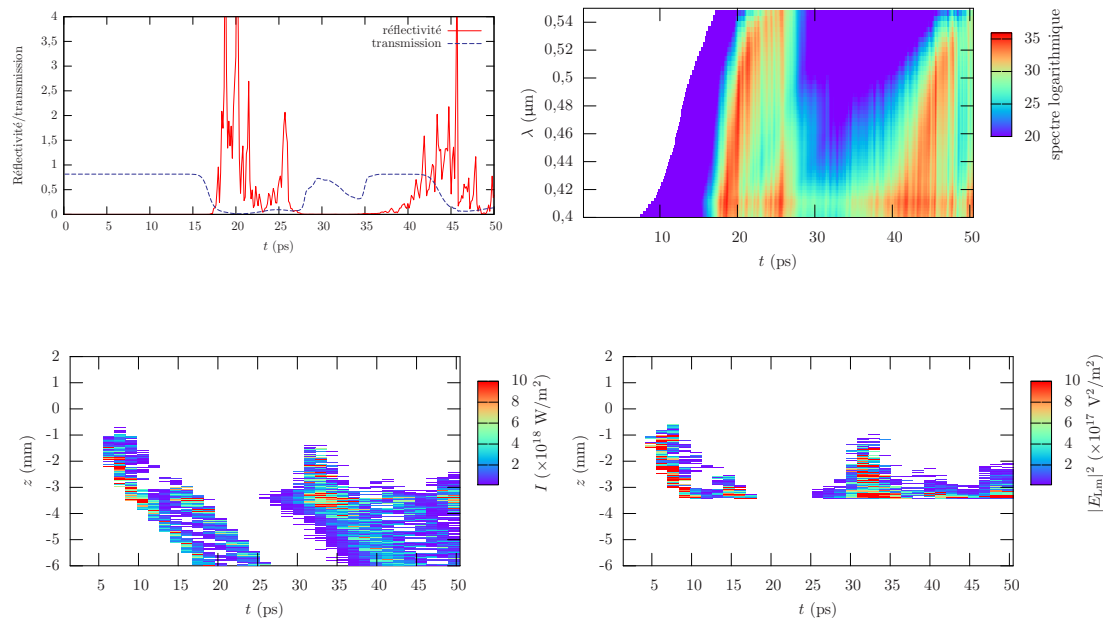


Figure 4: Nonlinear Raman backscattering simulation on the LIL plasma. On the top left, laser transmission and reflectivity vs time. On the top right, time-resolved scattered spectrum. On the bottom, streak view of the scattered (left) and of the Langmuir (right) waves.

spectrum curves (fig. 4) in which pump depletion is the source of a pulsed behaviour of the plasma response.

Acknowledgements

Authors thank D. Pesme and S. Hüller for helpful physical discussions.

References

- [1] Besnard D 2006 *Eur. Phys. J. D* e2006–00165–4
- [2] Morice O, Loiseau P, Teychenné D and Casanova M 2006 *J. Phys. IV France* **133** 325
- [3] Morice O and Casanova M 2007 IFSA conference, Kobe (Japan)
- [4] Garnier J *et al.* 2003 *JosaB* **20** 1409
- [5] Morales G J and O’Neil T M 1972 *Phys. Rev. Lett* **28**, 417
- [6] Krapchev V and Ram A 1980 *Phys. Rev. A* **22**, 1229